Effect of Nonhydrostatic Stress on Crystal Growth Kinetics

EFFECT OF NONHYDROSTATIC STRESS ON CRYSTAL GROWTH KINETICS

Michael J. Aziz, Paul C. Sabin, and Guo-Quan Lu[a], Division of Applied Sciences, Harvard University, Cambridge MA 02138

ABSTRACT

The effect of nonhydrostatic stresses on the solid phase epitaxial growth rate of crystalline Si(100) into self-implanted amorphous surface layers has been measured. Uniaxial stresses of up to 6 kbar (0.6 GPa) were attained by bending wafers over SiO_2 rods and annealing at a temperature too low for plastic deformation to relieve the stress in the crystal, but high enough for solid phase epitaxial growth to proceed. The growth rate on the tensile side was greater than that on the compressive side of the wafer, in marked contrast to the enhancement observed from hydrostatic pressure. The phenomenology of an "activation strain", the nonhydrostatic analogue of the activation volume, has been developed to characterize the results. Combined with the measurement of the activation volume, the measurement reported here permits us to characterize to first order the entire activation strain tensor corresponding to the transition state for solid phase epitaxy of Si(100). We conclude that the transition state for this process is "short and fat"; that is, the fluctuation to the transition state involves an expansion in the two in-plane directions and a contraction in the direction normal to the surface large enough to make the overall volume change negative. The symmetry of the measured activation strain tensor is inconsistent with all bulk point defect mechanisms for solid phase epitaxy. The relevance of the activation strain formalism to heteroepitaxy and vapor phase epitaxy is discussed.

INTRODUCTION

Nonhydrostatic stresses during crystal growth typically occur during strained-layer heteroepitaxy [1-3] or any other epitaxial growth process involving composition discontinuities or gradients. The effect of nonhydrostatic stress on phase stability is currently an area of active research [4-7]; here we address its effect on the interfacial or atomic mobilities. Although the effect of pressure on the kinetic rate constants for crystal growth have been studied [8-13], a measurement of the effect of nonhydrostatic stress states has proved elusive. This is due in part to the difficulty of imposing a controlled amount of nonhydrostatic stress without having it partially relieved and rendered, on a fine scale, non-uniform by dislocation injection.

In a study of the effect of pressure on quartz growth, Fratello *et al.* found evidence suggesting that nonhydrostatic stresses were even more effective in enhancing the growth rate than was pressure [4], but they were unable to control or quantify the nonhydrostaticity. Similarly, the solid phase epitaxy rate of crystalline Si (c-Si) into self-implantation-amorphized Si (a-Si) overlays is also enhanced by pressure [12,13]. We have measured the effect of nonhydrostatic stress on this rate, developed a theory for its consequences on an atomistic scale, and used the results to rule out a class of atomistic models for the solid phase epitaxy process [14,15]. The measurement was accomplished by elastically bending Si wafers over fused quartz rods at a temperature too low for plastic deformation to occur but high enough for solid phase epitaxial growth to proceed at measurable rates. The difference between the growth rates on the compressive and tensile sides of the wafer was measured, as was the behavior of the growth rate as the stress varied along the length of the wafer.

EXPERIMENT

Si (100) wafers (p-type, 1" diam., 1 Ω-cm, 0.033" thick, polished on both sides) were implanted on both sides at 77 K with $^{30}Si^+$ (60 keV, 1 x $10^{15}/cm^2$, <1.0 $\mu A/cm^2$, followed by 180 keV, 2 x $10^{15}/cm^2$, <1.3 $\mu A/cm^2$) to create amorphous surface layers 2800 Å thick. Wafers were diced into bars >20 mm long in the [011] direction, by 5 mm wide.

Mat. Res. Soc. Symp. Proc. Vol. 202. © 1991 Materials Research Society

Stress was imposed in air with a three-point bending system, depicted in Fig. 1. The sample rested on a pair of parallel fused quartz rods spaced 20 mm apart. A third fused quartz rod made contact with the sample from above. Weights were added to control the stress applied to the

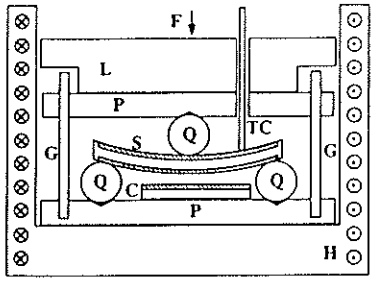

Fig. 1. Schematic cross section of three-point bending apparatus for annealing wafers under nonhydrostatic stress. S: sample, cross-hatched areas correspond to amorphous Si; C: calibration sample; Q: fused quartz support rods; P: brass plate; G guide posts; TC: thermocouple; H: heating element; F: weights; L: lid.

sample. An unstressed "calibration sample", which had only the top surface implanted, lay below the experimental sample; it served to calibrate temperatures and/or gradients.

The apparatus was pre-heated in the furnace to ~560°C. The top piece of the apparatus was removed and the sample and "calibration sample" were inserted quickly; this resulted in a temperature drop of slightly more than 20°C. Subsequently the temperature was stabilized at 540 ± 2°C within 8 minutes. Concurrently, the appropriate weight was completely added within 4 minutes. Typical anneal durations were 60 - 90 min. The sample was removed from the furnace as quickly as possible after the load had been removed, while it was still hot. After annealing, the thickness of the remaining a-Si layer was determined by Rutherford Backscattering Spectrometry and ion channeling [16] using 2 MeV $^4He^+$. The beam spot diameter was ~1.5 mm.

The stress state of the bar-shaped wafer in bending can be approximated as a uniaxial stress which varies linearly through the wafer thickness, with one side under compression and the other side under an equal amount of tension. Under the three-point bending load, the stress in the wafer also varies linearly from the single loading point at the center silica rod to the points of contact of the two supporting end rods. The magnitude of the stress is maximum on the wafer surface at the central loading point, and is zero at the point of contact of the two supporting end rods. At the wafer surface,

$$\sigma_{11}(x) = \pm \frac{|x| - L/2}{b\, h^2/3} F, \qquad (1)$$

where σ_{ij} is the stress tensor, x is the distance from the point of contact of the center rod, L is the length of the bar between the supporting end rods, F is the loading force on the bar, b is the width, and h is the thickness of the bar. All other σ_{ij} are zero in this approximation. The stress calculated from eq. (1) exists in the crystal at the crystal/amorphous interface. There is no stress in the bulk of the a-Si due to very rapid stress relief by viscous flow [17]. This was demonstrated by cooling down a sample while still loaded, after only a small amount of crystal growth. The sample retained its curvature when the load was removed. Upon annealing after the removal of the load, the sample straightened out again. Furthermore, that all samples stressed to >5 kbar during annealing broke into several pieces during careful removal of the load may be a consequence of flow.

The average growth rate for a sample whose maximum stress was σ_{11} = 6 kbar during an anneal at 540°C for 76 min. is shown in Fig. 2(a). The tensile side (dashed curve) grew faster and the compressive side (solid curve) of this wafer grew slower than did either side of two "control samples" (circles and triangles), which were annealed at low stress on separate runs in the same loading configuration as the high stress samples. The load on the control samples was not reduced all the way to zero, in order to maintain the same thermal contact between wafer and silica rods as in the high-stress sample. Note that the "control samples", unlike the "calibration samples", lie in the same place as the high-stress samples. The growth rates on the tensile and compressive sides approach each other as x = ± 10 mm, where the stress vanishes, is

approached. In Figs. 2(b) and (c) we show similar results for different wafers stressed to 6 kbar for 70 min. and 5 kbar for 60 min., respectively, at 540°C. In all cases, the difference between the growth rates on the tensile and compressive sides is maximum in the center of the wafer, where the stress difference is maximum.

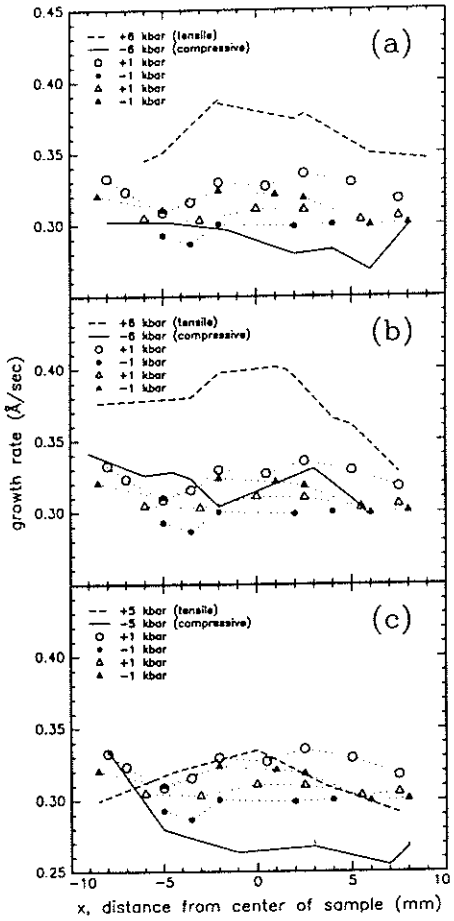

Fig. 2. Variation of average solid phase epitaxial growth rate at 540 °C with stress along length of bent wafer. Dashed line: tensile side of specimen; solid line: compressive side. In each case the magnitude of σ_{11}, indicated in the figure, is maximum in the center (x = 0), and varies linearly to zero at the ends (x = ± 10 mm). Dotted lines connect points taken from "control" samples under minimal load. Circles correspond to growth on opposite sides of one control sample; triangles to opposite sides of another. Differences between tensile and compressive sides of high stress samples are greatest in the center, where the stress difference is maximum, and lowest towards the ends, where stresses vanish.

DISCUSSION

The failure of the growth rates on the tensile and compressive sides to surround symmetrically the growth rates in the control samples is probably due to a small sample-to-sample variation in anneal temperature. However, the temperature difference between two sides of any particular wafer cannot be large enough to account for the difference in growth rates. The vertical temperature gradient in the 9-mm-high chamber was estimated to be no more than

0.7°C/mm by two methods. The first, which yielded a gradient of 0.3°C/mm, was by moving the thermocouple vertically through the chamber. The second, which yielded a gradient of 0.7°C/mm, was by measuring the simultaneous growth rate in the unstressed calibration sample lying at the bottom of the chamber in Fig. 1 and comparing to the average growth rate in the stressed sample. A calculation of the temperature gradient in the Si wafer, taking into account heat transfer by conduction and radiation and assuming the vertical heat flux to be constant

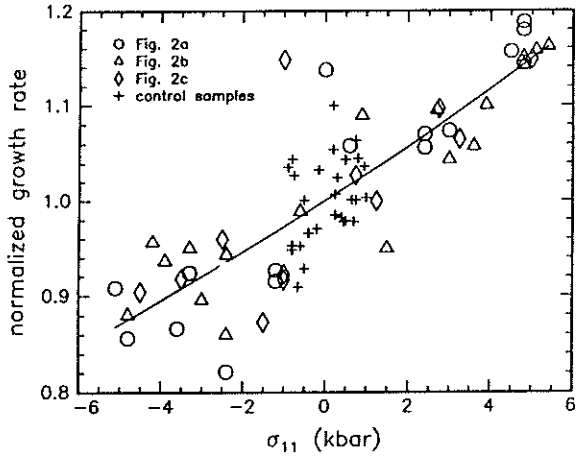

Fig. 3. Variation of average solid phase epitaxy rate with applied stress for all samples. Open symbols correspond to high stress samples in Fig. 2. The scatter in the data could be reduced by taking into consideration the controls and the trends evident from Fig. 2, but such manipulations are not necessary in order to obtain an approximate magnitude for the stress effect. Curve is fit to equation (2) with $\Delta V^*_{11} = 0.15\ \Omega$.

through both the silicon wafer and the surrounding air, indicates that the temperature difference between the tensile and compressive surfaces of the sample is less than 0.2°C. (The gradient is not large enough for convection to occur.) The effective temperature difference across the wafer that would account for the observed difference in growth rate is 6°C for the 6 kbar samples and 5°C for the 5 kbar sample. It is also possible that the a-Si layer becomes thinner on the tensile side, and thicker on the compressive side, by flow. The observed effect is over three times too large to be due to flow alone, even with sufficient flow to completely relax all stresses in the a-Si.

All data from Fig. 2 are divided by the best-fit zero-stress velocity for each sample, and plotted in Fig. 3 to display the effect of applied stress on the velocity. The curve fit to the data is derived from an extension of transition-state theory (TST) to nonhydrostatic stress states [9,18].

In TST, the probability of a fluctuation on the atomic scale from an initial configuration to a saddle-point in configuration-space (the "transition state") is evaluated. Stresses (hydrostatic or otherwise) applied to the surfaces of the wafer interact elastically with the fluctuating atomic configurations, biasing the fluctuation probabilities. In solid phase epitaxy, the velocity υ is proportional to the probability of fluctuating to the saddle point. TST gives familiar results for the activation energy $\Delta E^* = -k\partial(\ln \upsilon)/\partial(1/T)|_{p=0}$ and volume $\Delta V^* = -kT\partial(\ln \upsilon)/\partial P|_T$. Its extension to nonhydrostatic conditions yields $kT\partial(\ln \upsilon)/\partial\sigma_{ij} = \Delta V^*_{ij}$, or

$$\upsilon(\sigma_{ij}) = \upsilon(0)\ \exp \frac{\sigma^{appl}_{ij}\ \Delta V^*_{ij}}{kT}\ , \qquad (2)$$

where $\Delta V^*_{ij} \equiv V^*\ \overline{\varepsilon^*_{ij}}$, V^* is the initial volume of a volume element (the "subsystem") that surrounds the fluctuating atoms and encloses enough material so that all elastic behavior outside the volume element is linear, and $\overline{\varepsilon^*_{ij}}$ is the subsystem-volume-averaged value of ε^*_{ij}, the activation strain tensor, which takes the initial configuration into the saddle point.

When the curve in Fig. 3 is fit to equation (2) we find $\Delta V^*_{11} = (0.15 \pm 0.01)\ \Omega$, where Ω is the atomic volume of c-Si. Since symmetry requires that $\varepsilon^*_{22} = \varepsilon^*_{11}$ (these are the two in-plane directions), and since we have previously measured [12] the activation volume to be $\Delta V^* = -0.28\ \Omega$, which corresponds to the trace of ΔV^*_{ij}, we have $\Delta V^*_{33}/\Omega = -0.58$. Hence the transition state is "short and fat". That is, the fluctuation to the transition state involves an expansion in the two in-plane directions, coupled with a contraction in the direction normal to the surface large enough to make the overall volume change negative. Thus the probability of fluctuation to this state is enhanced by tension in either of the in-plane directions but is also enhanced by hydrostatic pressure. In our interpretation based on the most plausible atomistic mechanism of solid phase epitaxy [15] (the "interface dangling bond" mechanism of Spaepen and Turnbull [19]) the measured activation strain tensor would be the sum of a tensor describing dangling bond formation at the crystal/amorphous interface and a tensor describing dangling bond motion at the interface. We cannot separate the individual contributions of these two tensors from this experiment. However, the model's prediction of a negative volume of motion [20] is very encouraging.

From equation (1), we predict that (i) biaxial stress of the type normally encountered in heteroepitaxy will have the effect of uniaxial stress, squared; (ii) uniaxial compression in the direction normal to the surface will enhance the growth rate even more than does hydrostatic pressure. This explains the excessive magnitude of the apparent ΔV^* measured in a piston-cylinder high-pressure apparatus, in which a nonhydrostatic component of just this type might be expected, in an early experiment [16].

A measurement of ΔV^*_{ij} for any kinetic process provides a valuable constraint on proposed atomistic mechanisms of the process. For example, we used these results to rule out bulk point defect mechanisms for solid phase epitaxy [15].

These measurements, though made on a homoepitaxial process, are relevant to heteroepitaxy. They indicate that if solid phase epitaxy were performed under biaxial tensile stress, for example under conditions of coherence with a substrate with a larger lattice parameter, the stress effect would enhance the rate (although chemical effects might also play a rôle and the relative contributions of these and other effects would have to be sorted out). Conversely, in solid phase epitaxy performed under compressive biaxial stress, the stress would tend to retard the rate. This conclusion is consistent with that drawn by Paine *et al.* [21] in this symposium to explain the retardation of solid phase epitaxy rate of strained Si-Ge alloys on Si.

The effect that we have observed is small, but the maximum stress that we could attain without shattering the wafer (6 kbar, 0.6 GPa) was also quite small. In strained-layer heteroepitaxy, several tens of kilobars can be attained. Combined with the predicted exponential stress-dependence and the enhancement due to biaxiality discussed above, significantly larger effects might be observed in strained-layer heteroepitaxy.

Although the atomistic mechanism might be different, the same "activation strain" formalism is valid for vapor phase epitaxy. Measurements of the activation strain tensor might place constraints on proposed atomistic mechanisms. We expect that the transition state for this process may interact elastically with the surroundings through wafer bending, lattice mismatch, and surface stresses. Furthermore, an adsorbate might catalyze crystal growth elastically through its effect on the surface stress [22,23]. The activation strain effect presents opportunities for finding new pathways to low-temperature epitaxial growth.

SUMMARY

We have measured the effect of uniaxial stress on the kinetics of crystal growth. Solid phase epitaxy is enhanced by uniaxial tension but is also enhanced by hydrostatic compression. The results are interpreted in terms of an extension of transition state theory to nonhydrostatic stress states. The explanation is that the probability of a fluctuation to a transition state with a "short and fat" activation strain tensor would be enhanced by in-plane tension, or by compression normal to the surface. A measurement of the activation strain tensor provides a means of testing proposed atomistic mechanisms; we have used this to rule out a class of proposed mechanisms of solid phase epitaxy. Vapor phase epitaxy is one example of the array of other kinetic processes involving stressed solids for which the activation strain formalism should apply.

ACKNOWLEDGEMENTS

We are grateful to K.-R. Lee and J.F. Chervinsky for technical assistance with RBS, to A. Witvrouw for performing curvature measurements, and to J.R. Rice, F. Spaepen, H.A. Stone, and J.A. Golovchenko for helpful discussions. Samples were implanted at the Surface Modification and Characterization Facility at Oak Ridge National Laboratory. This research was supported by NSF-DMR-89-13268. One of us (P.C.S.) was supported jointly by the Undergraduate Faculty Aide Program, the Materials Research Laboratory (NSF-DMR-89-20490), and the Division of Applied Sciences at Harvard University.

REFERENCES

[a] Present address: Alcoa Technical Center, 7th Street Road, Route 780, Alcoa Center, PA 15069.

[1] J.Y. Tsao, B.W. Dodson, S.T. Picraux and D.M. Cornelison, Phys. Rev. Lett. 59, 2455 (1987).

[2] J.W. Matthews and A.E. Blakeslee, J. Cryst. Growth 27, 118 (1974).

[3] B.T. Chilton, B.J. Robinson, D.A. Thompson, T.E. Jackman, and J.-M. Baribeau, Appl. Phys. Lett. 54, 42 (1989).

[4] F.C. Larché and J.W. Cahn, Acta Metall. 33, 331 (1985).

[5] P.W. Voorhees and W.C. Johnson, J. Chem. Phys. 84, 5108 (1986).

[6] P.W. Voorhees and W.C. Johnson, Phys. Rev. Lett. 61, 225 (1988).

[7] P.H. Leo, W.W. Mullins, R.F. Sekerka, and J. Viñals, Acta Metall. Mater. 38, 1573 (1990).

[8] V.J. Fratello, J.F. Hays, and D. Turnbull, J. Appl. Phys. 51, 4718 (1980).

[9] M.J. Aziz, E. Nygren, J.F. Hays and D. Turnbull, J. Appl. Phys. 57, 2233 (1985).

[10] G. Devaud, M.J. Aziz, and D. Turnbull, J. Non-Cryst. Sol. 109, 121 (1989).

[11] E. Chason and M.J. Aziz, submitted to J. Non-Cryst. Sol.

[12] G.Q. Lu, E. Nygren, M.J. Aziz, D. Turnbull and C.W. White, Appl. Phys. Lett. 54, 2583 (1989).

[13] G.Q. Lu, E. Nygren, M.J. Aziz, D. Turnbull and C.W. White, Appl. Phys. Lett. 56, 137 (1990).

[14] M.J. Aziz, P.C. Sabin, and G.-Q. Lu, submitted to Phys. Rev. Lett.

[15] G.-Q. Lu, E. Nygren, and M.J. Aziz, Mat. Res. Soc. Symp. Proc. 205 (in press, 1991).

[16] E. Nygren, M.J. Aziz, D. Turnbull, J.M. Poate, D.C. Jacobson, and R.Hull, Appl. Phys. Lett. 47, 232 (1985).

[17] A. Witvrouw and F. Spaepen, Mat. Res. Soc. Symp. Proc. 205 (in press, 1991)

[18] M.J. Aziz, to be published.

[19] Spaepen and Turnbull, AIP Conf. Proc. 50, 73 (1979).

[20] V.J. Fratello, J.F. Hays, F. Spaepen, and D. Turnbull, J. Appl. Phys. 51, 6160 (1980).

[21] D.C. Paine, D.H. Howard, N.Evans, D.J. Greve, M. Racanelli, and N.G. Stoffel, Mat. Res. Soc. Symp. Proc. 202 (in press, 1991).

[22] R.D. Meade and D. Vanderbilt, Phys. Rev. Lett. 63, 1404 (1989).

[23] R.E. Martinez, W.M. Augustyniak, and J.A. Golovchenko, Phys. Rev. Lett. 64, 1035 (1990).